

1 **Physiological and biochemical responses of *Emiliana huxleyi* to**
2 **ocean acidification and warming are modulated by UV radiation**

3 Shanying Tong^{1,3}, David A. Hutchins², Kunshan Gao¹

4 ¹State Key Laboratory of Marine Environmental Science, Xiamen University, Xiamen,
5 China

6 ²Department of Biological Sciences, University of Southern California, Los Angeles,
7 California, USA

8

9 ³College of Life Science, Ludong University, Yantai, China

10

11 Correspondence to: Kunshan Gao (ksgao@xmu.edu.cn)

12

13

14

15

16

17

18

19

20

21

22

23

24

25 **Abstract**

26 Marine phytoplankton such as bloom-forming, calcite-producing coccolithophores,
27 are naturally exposed to solar UV radiation (UVR, 280-400 nm) in the ocean's upper
28 mixed layers. Nevertheless, effects of increasing CO₂-induced ocean acidification and
29 warming have rarely been investigated in the presence of UVR. We examined
30 calcification and photosynthetic carbon fixation performance in the most
31 cosmopolitan coccolithophorid, *Emiliana huxleyi*, grown under high (1000 µatm, HC;
32 p_{H_T}: 7.70) and low (400 µatm, LC; p_{H_T}: 8.02) CO₂ levels, at 15 °C (LT), 20 °C (MT)
33 and 24 °C (HT) with or without UVR. The HC treatment didn't affect photosynthetic
34 carbon fixation at 15 °C, but significantly enhanced it with increasing temperature.
35 Exposure to UVR inhibited photosynthesis, with higher inhibition by UVA (320-395
36 nm) than UVB (295-320 nm), except in the HC and 24 °C-grown cells, in which UVB
37 caused more inhibition than UVA. Reduced thickness of the coccolith layer in the
38 HC-grown cells appeared to be responsible for the UV-induced inhibition, and an
39 increased repair rate of UVA-derived damage in the HCHT-grown cells could be
40 responsible for lowered UVA-induced inhibition. While calcification was reduced
41 with the elevated CO₂ concentration, exposure to UVB or UVA affected it
42 differentially, with the former inhibiting and the latter enhancing it. UVA-induced
43 stimulation of calcification was higher in the HC-grown cells at 15 and 20 °C,
44 whereas at 24 °C, observed enhancement was not significant. The calcification to
45 photosynthesis ratio (Cal/Pho ratio) was lower in the HC treatment, and increasing
46 temperature also lowered the value. However, at 20 and 24 °C, exposures to UVR
47 significantly increased the Cal/Pho ratio, especially in HC-grown cells, by up to 100%.
48 This implies that UVR can counteract the negative effects of the 'greenhouse'
49 treatment on the Cal/Pho ratio, and so may be a key stressor when considering the

50 impacts of future greenhouse conditions on *E.huxleyi*.

51

52 **Key words:** *Emiliana huxleyi*, ocean acidification, temperature, UV radiation,

53 photosynthesis, calcification

54

55 **1 Introduction**

56 Coccolithophores are a group of calcifying unicellular phytoplankton within the
57 Prymnesiophyceae (Paasche, 2002). They are an ecologically and biogeochemically
58 prominent marine phytoplankton functional group, and contribute to carbon dioxide
59 sinks and sources by performing both photosynthesis and calcification, respectively
60 (Raitsos et al., 2006; Raven and Crawford, 2012). Although the ballasting of
61 photosynthetic products by coccoliths helps to efficiently transport carbon from the
62 photic zone, the calcification process is a net source of CO₂ to the environment (Rost
63 and Riebesell, 2004; Gattuso et al., 1996). Therefore, the ratio of photosynthesis to
64 calcification determines their net contribution to carbon dioxide uptake or release.
65 Consequently, investigating changes in these two processes under varying
66 environmental conditions is a key to our understanding of their biogeochemical roles
67 under ocean global change. Calcification and photosynthesis of coccolithophores are
68 influenced by many factors, including nutrients, light availability, and CO₂, as well as
69 temperature and ultraviolet radiation (UVR) (Riebesell et al., 2017; Tong et al.,
70 2016; Feng et al., 2008).

71 Rising atmospheric CO₂ concentration due to human activities causes greenhouse
72 warming of the atmosphere and ocean, and the dissolution of this anthropogenic CO₂
73 into the surface ocean reduces the pH of seawater in a process known as ocean
74 acidification (OA). Ongoing OA has been predicted to decrease pH by 0.40 units in

75 pelagic waters (Gattuso et al., 2015) and by 0.45 (Cai et al., 2011) units in coastal
76 waters (Cai et al., 2011) by the end of this century under the business-as-usual CO₂
77 emissions scenario. On the other hand, increased atmospheric CO₂, along with other
78 greenhouse gases, will warm the Earth's surface by 2.5-6.4 °C by the year 2100
79 (Alexiadis, 2007), while the surface ocean temperature is projected to rise by 2-3 °C
80 (Stocker et al., 2014). Most previous work has indicated that warming enhances
81 stratification (Capotondi et al. 2012), although this has recently been disputed
82 (Somavilla et al. 2017). Assuming that ocean warming is shoaling the depth of the
83 upper mixed layer (UML), this would affect the integrated levels of
84 photosynthetically active radiation (PAR) and ultraviolet radiation (UVR) to which
85 phytoplankton cells within the UML are exposed (Häder and Gao, 2015). Regardless,
86 increasing concentrations of CO₂ and other greenhouse gases will also begin to play
87 an ever-increasing role in determining levels of cloud cover and stratospheric ozone,
88 thus affecting the amount of UVR reaching ocean surface (Williamson et al., 2014).

89 All these ocean global changes may have individual and/or interactive effects on
90 the physiology of marine primary producers (Hutchins and Fu, 2017;Gao et al., 2012) .
91 OA usually decreases calcification of *E. huxleyi*, although corresponding pCO₂
92 increases can enhance photosynthesis or growth at the same time (Riebesell et al.,
93 2017;Riebesell et al., 2000). Under nutrient replete conditions, increased light levels
94 appear to counteract the negative impacts of OA on calcification on *E. huxleyi* (Jin et
95 al., 2017). The calcified coccoliths are thought to play roles in protections against
96 grazing pressure, viral and bacterial attack (Monteiro et al., 2016), and can also help
97 protect cells from UV radiation (Gao et al., 2009) . Early experiments on *E. huxleyi*
98 strain BT-6 showed that cells had a complete covering of coccoliths at 12.5 to 23 °C,

99 but at 26.5 °C, 30% of the cells had an incomplete covering (Paasche, 1968).
100 Similarly, Langer et al. (2009) saw increased malformed coccoliths in *E. huxleyi* RCC
101 1238 at 25 °C compared to those grown at 20 and 10 °C . A recent study showed that
102 increased temperature aggravates the impacts of OA on *E. huxleyi* morphology
103 (Milner et al., 2016).

104 Increasing levels of PAR or temperature and changes in UVR and nutrient
105 availability may interact with each other to cause additive, antagonistic or synergistic
106 effects on coccolithophores. Nevertheless, most previous studies have been carried
107 out under PAR only, without UVR or fluctuating solar radiation being considered.
108 However, UVR cannot be ignored when examining the effects of environmental
109 changes on marine phytoplankton that are found in the upper half of the euphotic zone,
110 since UV irradiance can penetrate as deep as 80 m in pelagic waters (Tedetti et al.,
111 2007). Excessive solar UV-B and UV-A can damage DNA and interfere with many
112 cellular biochemical processes (Häder et al., 2014). On the other hand, moderate
113 levels of UVA can enhance photosynthetic carbon fixation of phytoplankton
114 assemblages (Gao et al., 2007; Helbling et al., 2003). As for UVR effects on
115 coccolithophore calcification, recent studies demonstrated that the outer coccoliths of
116 *E. huxleyi* can effectively shield the cells from a certain percentage of UVR radiation
117 (Xu et al., 2016). Nevertheless, the transmitted energy still causes significant
118 inhibition of calcification, as well as photosynthesis (Gao et al., 2009). Exposure of *E.*
119 *huxleyi* to solar UV radiation decreased its growth rate, but increased its production of
120 coccoliths per cell (Guan and Gao, 2009).

121 Since exposure to solar UV radiation can influence cytoplasmic redox activities
122 (Wu et al., 2010), and inhibit or enhance physiological performances at different
123 levels of UVR, we hypothesized that effects of OA and warming on coccolithophores
124 would be different with and without the presence of UVR. To test our hypothesis, in
125 this study we examined the responses of *E. huxleyi* photosynthesis and calcification to
126 OA with or without UVR at three temperature levels.

127

128 **2. Materials and methods**

129 **2.1 Experimental setup**

130 Experiments used *Emiliana huxleyi* strain PML B92/11, originally isolated from the
131 field station of the University of Bergen, Norway (Raunefjorden; 60 °18'N, 05 °15'E).
132 To first test interactions between OA and temperature, thermal reaction curves were
133 obtained by growing the cultures at 15, 20, 22, 24 and 27 °C in artificial seawater
134 pre-equilibrated with elevated (1000 µatm, HC) or ambient (400 µatm, LC)
135 atmospheric CO₂ concentrations. Triplicate experimental cultures were maintained
136 without aeration under PAR (cool-white fluorescent lamps) of 190 µmol m⁻²s⁻¹ with a
137 12/12 light/dark cycle. The culture medium was enriched with 100 µmol l⁻¹ nitrate and
138 10 µmol l⁻¹ orthophosphate, and vitamins and trace metals were added according to
139 the Aquil recipe (Sunda et al., 2005). The maximum cell concentration in all
140 treatments was maintained below 5 × 10⁴ cells ml⁻¹ in order to maintain stable
141 carbonate chemistry (pH variation < 0.04). After the cells were grown in each
142 treatment for about 10 generations, the growth rates were determined. Then the
143 thermal reaction norms were plotted for HC- and LC-grown cells according to the
144 equation:

$$145 \quad f(T) = ae^{bT} \left[1 - \left(\frac{T-z}{w/2} \right)^2 \right] \quad (1),$$

146 where w is the temperature niche width, z is the midpoint of the growth curve, and b
147 and a jointly determine the overall steepness, height, and skewness of the curves
148 (Thomas et al., 2012; Norberg, 2004). The optimum temperature for growth (T_{opt}) was
149 estimated from the fitted curve by numerical optimization.

150 Based on T_{opt} from the thermal curve, 15, 20 and 24 °C were selected to grow the
151 cells for another 10 generations. The rationale for choosing these temperatures is that
152 15 and 20 °C are below and close to the optimal growth temperature, while 24 °C is
153 above it. To investigate how the cells responded to these three different levels of
154 temperature and two pCO₂ levels in the presence of transient UV irradiance exposures
155 such as might be encountered by cells in a dynamic mixed layer, they were then
156 exposed to the different radiation treatments for three hours before photosynthesis and
157 calcification parameters were measured (section 2.2.3).

158

159 **2.2 Measurements and analysis**

160 **2.2.1 Growth rates**

161 The specific growth rates (μ) were determined from cell counts performed with a Z2
162 Coulter Counter (Beckman, Buckinghamshire, UK), calculated using the equation: $\mu =$
163 $(\ln C_1 - \ln C_0) / (t_1 - t_0)$, where t_0 and t_1 were the times of inoculation and sampling, $t_1 -$
164 t_0 was the interval between inoculation and sampling, and C_0 and C_1 were the cell
165 concentrations at time t_0 and t_1 .

166

167 **2.2.2 POC, PON and PIC analysis and estimation of inner coccosphere volume**

168 After cells were cultured at 15, 20, and 24 °C for another 10 generations, duplicate
169 samples (200 mL) taken in the middle of the light period were filtered onto 25 mm
170 precombusted (450 °C for 6h) Whatman GF/F filters and stored at -20 °C. For

171 analysis, one of the duplicate filters for each treatment was fumed over HCl for 12h to
172 remove inorganic carbon and then dried overnight at 60 °C; the other filters were
173 dried overnight at 60 °C directly. All the filters were then packed in tin cups and
174 analyzed on a Perkin Elmer Series II CHNS/O Analyzer 2400. PIC was determined by
175 the difference between TPC (total particulate carbon) and POC. The production rates
176 of POC or PIC were calculated as $P = \text{cellular POC or PIC content (pg cell}^{-1})$
177 $\times \text{specific growth rate } \mu \text{ (d}^{-1})$

178 The inner coccosphere (protoplast) volume (V_{cell}) were calculated according to:

$$179 \quad \frac{\text{POC[pg]}}{\text{cell}} = a \times V_{\text{cell}}^b \quad (2)$$

180 Where a (0.216 in this case) and b (0.939 in this case) are constants which vary
181 depending on the investigated species (Menden-Deuer and Lessard, 2000).

182 **2.2.3 Radiation treatment and determination of calcification and photosynthetic** 183 **rates**

184 Right before the samples for elemental analysis were taken, the cells acclimated to
185 each temperature and pCO₂ level were dispensed into 100 ml quartz tubes (volume 90
186 ml) and inoculated with 5μCi (0.185 MBq) of labeled sodium bicarbonate (ICN
187 Radiochemicals). The quartz tubes (n=3) were then exposed to a solar simulator with
188 PAR, UVA and UVB irradiance levels of 42 W m⁻² (190 μmol m⁻²s⁻¹), 13.5 W m⁻², and
189 0.81 W m⁻², respectively. The radiation intensity was measured using a three channel
190 irradiation apparatus (PMA2100, Solar Light). The PAR used was equivalent to the
191 mean light level in the upper mixed layer (UML) based on time series station (19 °N,
192 118.5 °E) measurements in the South China Sea (Chen et al., 2006). The ratios of
193 both UVA and UVB to PAR emitted by the solar simulator were about 30% higher
194 than those of the sunlight reaching the sea surface. The following three radiation
195 treatments were realized: PAR+UVA+UVB (PAB), quartz tubes covered with 295 nm

196 cut-off film (Ultraplan, Digefra), so that the cells were exposed to irradiances above
197 295 nm; PAR+UVA (PA), covered with 320 nm cutoff film (Montagefolie, Folex),
198 with the cells exposed to irradiances above 320 nm; and PAR (P), covered with 395
199 nm cutoff film (Ultraplan UV Opak, Digefra), so that the cells received irradiances
200 above 395 nm. The temperatures were controlled with a cooling circulator (CAP-3000,
201 Rikakikai, Japan). The exposure duration lasted for 3h, and each treatment had 3
202 replicates for the incubations. This short exposure period under the solar simulator
203 can mimic mixing of cells to the surface or the reappearance of sunlight after
204 cloudiness, both of which occur frequently in nature.

205 The collected samples from each treatment were immediately filtered onto
206 Whatman GF/F filters (25mm), rinsed with unlabeled medium, and then put in 20 ml
207 scintillation vials. One filter from each tube was fumed over HCl overnight to remove
208 the coccolith coverage, and then dried at 45 °C for 4 h to estimate the photosynthetic
209 carbon fixation rate, while other filters were dried directly to estimate the total carbon
210 fixation rate. 3.5 ml scintillation cocktail (Perkin Elmer) were added to the vials, and
211 all the filters were counted using a liquid scintillation counter (LS6500 Multi-Purpose
212 Scintillation Counter, Beckman Counter, USA). The rate of calcification was
213 determined as the difference between total and photosynthetic carbon fixation rate.
214 The inhibition of calcification and photosynthesis due to UVA, UVR, or UVB was
215 calculated as:

$$216 \text{Inh}_{\text{UVA}} = (R_P - R_{\text{PA}}) / (R_P) \times 100\%$$

$$217 \text{Inh}_{\text{UVR}} = (R_P - R_{\text{PAB}}) / (R_P) \times 100\%$$

$$218 \text{Inh}_{\text{UVB}} = (R_{\text{PA}} - R_{\text{PAB}}) / (R_P) \times 100\% = \text{Inh}_{\text{UVR}} - \text{Inh}_{\text{UVA}}$$

219 Where R_P , R_{PA} , and R_{PAB} represented the rate of calcification or photosynthesis under
220 PAR, PAR+UVA and PAR+UVA+UVB respectively.

221 **2.2.4 Estimation of carbonate chemistry**

222 The pH of the seawater was measured with a pH meter (Benchtop pH510, Oakton)
223 that was calibrated with standard NBS (National Bureau of Standards) buffer. The
224 CO₂ concentration of the aeration was monitored with a CO₂ meter (Vaisala, GM70)
225 with variations < 4%. The cell concentrations of all cultures were maintained below
226 5×10^4 cells ml⁻¹ to make sure pH variations were <0.04 units. Other seawater
227 carbonate system parameters were calculated with the CO2SYS software using the
228 known parameters of pCO₂, salinity, pH, temperature and nutrient concentrations
229 (Lewis et al., 1998). The carbonic acid dissociation equilibrium constants K₁ and K₂
230 were determined according to Roy et al. (1993) and that for boric acid was from
231 Dickson (1990).

232 **2.2.5 Data Analysis**

233 Before parametric tests were performed, data were tested for homogeneity of variance
234 and normality. Two-way or three-way analysis of variance (ANOVA) were used to
235 establish differences among the treatments. Then post-hoc multiple comparisons were
236 used to determine significant differences between temperature, CO₂ or UV treatments.
237 Significance levels were set at p<0.05.

238 **3 Results**

239 **3.1 Thermal reaction norms**

240 The growth temperature curve (growth thermal norms) obtained for *E. huxleyi* (Fig. 1)
241 exhibited different shapes in the LC and the HC-grown cells. The LC cultures showed
242 an asymmetric pattern that is common to many algal species, in which the growth rate
243 increased with rise of temperature to reach a maximum of 1.3 d⁻¹ at 22.2 °C and then
244 declined sharply at temperatures above this optimal point. At 20 and 24 °C, growth
245 rate was <10% lower compared to 22.2 °C, so 20 and 24 °C were still within the

246 optimal growth temperature range for LC-grown *E. huxleyi*. The HC-grown cells
247 showed a relatively symmetric thermal norm, with an optimal growth temperature at
248 20.6 °C, 1.6 °C lower than that of the LC-grown ones. Thus the growth rate at 20 °C
249 was near maximal, while the value at 24 °C decreased by nearly 20% compared to the
250 maximal growth rate. The net effect of these trends was that growth rate of the
251 LC-grown cells was significantly ($p < 0.05$) higher than that of the HC-grown cells at
252 22 and 24 °C (Fig. 1).

253 **3.2 Growth rate**

254 During the 10 generations of growth at two CO₂ levels and three temperatures prior to
255 the UV exposure, the growth rate was lowest at 15 °C and was further reduced by
256 17.4% in HC-grown cells compared to LC-grown ones ($p < 0.05$, Fig. 2). At 20 °C,
257 there was no difference in growth rates between HC- and LC-grown cells ($p > 0.05$). At
258 24 °C, growth rate didn't change in LC-grown cells ($p > 0.05$), but decreased in
259 HC-grown ones compared to that at 20 °C, and thus the value was 17.5 % lower in
260 HC-grown cells compared to LC-grown ones at 24 °C ($p > 0.05$).

261 **3.3 Cellular PIC and POC quotas, production rates and inner coccosphere** 262 **volumes**

263 The two CO₂ treatments had no effect on cellular POC content at 15 °C and 20 °C.
264 However, at 24 °C, the HC treatment significantly increased cellular POC by 18.4%
265 compared to the LC treatment ($p < 0.01$, Fig. 3a), yielding the highest value among the
266 treatments. Cellular PIC content was reduced with increased CO₂ concentration in the
267 15, 20, and 24 °C treatments by 35.8% ($p < 0.05$, Fig. 3b), 62.6% ($p < 0.05$) and 17.1%
268 ($p < 0.01$), respectively. In LC-grown cells, cellular PIC was significantly affected by
269 temperature, being the highest at 15 °C, and was decreased by 34.2% ($p < 0.01$) at
270 20 °C and 18.9% ($p < 0.01$) at 24 °C. In HC-grown cells, cellular PIC was 45.2 %

271 (p<0.01) and 41.7% (p<0.01) lower at 20 °C, compared to at 15 and 24 °C,
272 respectively. The production rate of POC ranged from 6.8 to 13.2 pg cell⁻¹d⁻¹ among
273 different treatments (Fig. 3c). At 15 °C, the HC treatment reduced POC production
274 rate by 26.6% (p<0.05), and the values were 42% (p<0.01) and 30% (p<0.01) lower in
275 HC- and LC-grown cells respectively compared to those at 20 °C. No significant
276 differences were observed between different CO₂ treatments at 20 °C and 24 °C
277 (p>0.05), and the temperature rising from 20 to 24 °C also had no significant effect on
278 POC production rate both in HC- and LC-grown cells (p>0.05). The HC treatment
279 lowered the PIC production rate by 42.3% (p<0.01, Fig. 3d), 37.3% (p<0.01), and
280 29.9% (p<0.01) at 15, 20, and 24 °C respectively. A 5 °C temperature decrease from
281 20 °C had no significant effect on PIC production rate both in LC- and HC-cultures
282 (p>0.05). However, a 4 °C increase from 20 to 24 °C enhanced the PIC production rate
283 by 41.9% (p<0.05) and 27.4% (p<0.05) in HC- and LC-grown cells respectively.

284 The pattern of inner coccosphere volume among different treatments was similar to
285 that of cellular POC (Fig. 3e), with a significantly higher value in HC-cultures than
286 LC-ones at 24 °C (p<0.01), while no difference existed between different CO₂
287 treatments at the other temperature levels (p>0.05).

288 The PIC to POC ratio (PIC/POC) had the lowest value at 20 °C in the HC treatment
289 (Fig. 3f), and the highest value at 15 °C in the LC treatment. Either reduced or
290 elevated temperature from 20 °C increased the PIC/POC ratio in both HC- and
291 LC-cultures (p<0.05), although the extent varied.

292 **3.4 Cellular PON content and POC/PON (C/N) ratio**

293 Cellular PON had the same trends between the HC and LC treatments at 15 and 20 °C
294 (p>0.05, Fig. 4a). Similar to cellular POC, at 24 °C cellular PON was 29.6% higher in
295 HC-grown cells compared to LC-grown ones (p<0.01).

296 The C/N ratio showed no significant difference among different temperatures in the
297 HC treatment ($p>0.05$, Fig. 4b). In the LC treatment, the C/N ratio was significantly
298 higher at 24 °C than that at 15 and 20 °C ($p<0.05$). The C/N ratio in the LC treatment
299 was 9.5% higher than that in the HC treatment at 24 °C ($p<0.05$), while the value
300 showed no significant difference between HC and LC treatment at 15 and 20 °C
301 ($p>0.05$).

302

303 **3.5 Responses of photosynthetic carbon fixation to UV radiation**

304 After 3 h of exposure under the solar simulator, significant interactive effects between
305 temperature and irradiance ($p<0.01$), temperature and $p\text{CO}_2$ ($p<0.01$), and irradiance
306 and $p\text{CO}_2$ ($p=0.042$) were observed on photosynthetic carbon fixation. There were no
307 differences in photosynthetic carbon fixation rates between HC- and LC-cultures at
308 15 °C under the PAR alone treatment ($p>0.05$, Fig. 5a), while the values were
309 marginally ($p=0.064$, Fig. 5b) and significantly higher ($p=0.026$, Fig. 5c) in
310 HC-grown cells compared to LC-grown ones at 20 and 24 °C. At 15 °C, presence of
311 UVA or UVR (UVA+UVB) had no significant effects on photosynthetic rate under the
312 LC conditions ($p>0.05$), however, it lowered the photosynthetic rate under the HC
313 conditions ($p<0.01$, Fig. 5d). At 20 °C, the values were reduced by 33.4% ($p<0.05$)
314 and 19.9% ($p=0.05$) in HC- and LC-grown cells under the PA treatment compared to
315 the PAR alone treatment (Fig. 5b, e). The PAB treatment didn't further lower the
316 photosynthetic rates compared to the PA treatment in either the HC- or LC-cultures
317 ($p>0.05$). At the highest temperature of 24 °C, the photosynthetic rate was 22.6%
318 ($p<0.01$) and 34.8% ($p<0.01$) lower under the PA treatment compared to the PAR
319 alone treatment in HC- and LC-grown cells respectively (Fig. 5c, f). The values were
320 further decreased by 35.7% ($p<0.01$) in HC-grown cells, but weren't affected in

321 LC-grown ones in the PAB treatment ($p>0.05$).

322 **3.6 Calcification rates and Cal/Pho ratios in response to UV exposures**

323 Calcification rates were significantly lower in HC-grown cells compared to
324 LC-grown ones under the PAR alone treatment at all temperature levels ($p<0.01$, Fig.
325 6 a, b, c). The PA treatment significantly increased the calcification rate in HC-grown
326 cells relative to the PAR alone treatment by 31.7% (Fig. 6a, d), 18.9% (Fig. 6b, e) and
327 30.3% (Fig. 6c, f) at 15, 20 and 24 °C respectively ($p<0.05$). However, there were no
328 significant differences in calcification rates between PA and PAR treatments in
329 LC-grown cells ($p>0.05$). Under the PAB treatment, the presence of UVB led to a
330 reduced calcification rate compared to the PA treatment at 15 °C ($p<0.01$). This
331 inhibition was significantly higher in HC- compared to LC-cultures (Fig. 6a, d), but
332 there were no significant differences in calcification rates between PA and PAB
333 treatments at 20 and 24 °C ($p>0.05$) in either HC- or LC-grown cells. There were
334 significant interactions between temperature and irradiance on calcification rate
335 ($p=0.018$).

336 Calcification to photosynthesis ratio (Cal/Pho ratio) values were significantly
337 higher under PA than in the PAR alone treatment ($p<0.05$, Fig. 6g, h, i), regardless of
338 the CO₂ concentrations and temperature levels. The Cal/Pho ratio was lower at 15 °C
339 under PAB compared to the PA treatment in both HC- ($p<0.01$) and LC-grown cells
340 ($p<0.05$), while there were no significant differences between those irradiance
341 treatments at 20 °C and 24 °C ($p>0.05$). Except in the PA treatment at 15 °C, the
342 Cal/Pho ratio was significantly lower in HC-grown cells compared to LC-grown ones
343 under all the other conditions, with the greatest reduction of 44.3% at 24 °C. There
344 were significant interactions among all three variables for the Cal/Pho ratio ($p<0.01$).

345

346 **4 Discussion**

347 Our results demonstrated that both photosynthesis and calcification were inhibited by
348 UVB. In contrast, UVA was more inhibitory for photosynthesis than UVB, while it
349 had a positive effect on calcification. The degree to which UVA and UVB affected the
350 performance of photosynthesis and calcification varied depending on CO₂
351 concentrations and temperature levels. Of the three temperature levels used, 15 °C
352 was much lower than optimal growth temperature for both HC- and LC- grown cells.
353 For LC cultures, the growth rate was the same at 20 and 24 °C, and those two
354 temperatures were in the optimal range for cells growth. While 20 °C was very close
355 to the optimal temperature for HC-grown cells, the growth rate at 24 °C was
356 significantly reduced, suggesting the cells growth at this temperature may be already
357 thermally inhibited. The different growth state among the three temperature levels,
358 particularly that between HC- and LC-grown cells at the highest temperature,
359 potentially affected the photosynthetic and calcification responses to UV radiation.

360 In this study, the inhibition of photosynthesis by UVA, UVB and their combination
361 appeared to increase with temperature. On the contrary, previous studies conducted on
362 other phytoplankton species such as diatoms suggested that increasing temperature
363 could reduce UV-induced inhibition of photosynthesis, as the activities of repair
364 associated enzymes are temperature dependent (Li et al., 2012; Helbling et al., 2011).
365 These differing trends between the present and previous studies may be attributed to
366 either changes in the thickness of the coccolith layer surrounding the cells, or to the
367 temperature range used. The coccoliths of *E. huxleyi* can provide a protective role
368 against UVR either by strongly scattering light, or by physically shading intracellular
369 organelles (Xu et al., 2016; Voss et al., 1998). In our results, the cellular PIC at 20 °C
370 was only half of that at 15 °C. Since cellular PIC is an indicator of the amount of

371 coccoliths on the exterior of the cell, this suggests that the cells grown at 20 °C had a
372 substantially thinner coccolith layer and so received much more UV radiation, leading
373 to increased photosynthetic damage compared to cells grown at 15 °C. At 24 °C, the
374 thermal reaction curves suggested that this temperature level was already close to the
375 upper tolerance limit for growth in *E. huxleyi* PML B92/11, with HC-grown cells
376 suffering more thermal stress. At this temperature, though the thickness of coccolith
377 layer was equal to that at 15 °C, biochemical aspects of UVR defense and /or repair
378 mechanisms may be under thermal stress (Sobrino and Neale, 2007).

379 At 15 and 20 °C the inhibition of photosynthesis was mainly caused by UVA, and
380 the values were significantly higher in HC-grown cells compared to LC-grown ones,
381 due to a thinner coccolith layer on cells in acidified seawater (Gao et al., 2009). In
382 contrast, at 24 °C the HC treatment alleviated the UVA-induced inhibition compared
383 to the LC treatment but also greatly enhanced inhibition by UVB. The underlying
384 mechanism may be protein-mediated defense/repair processes. This is supported by
385 the fact that the C/N ratio was increased by the LC treatment only at 24 °C. The C/N
386 ratio can reflect the defense and repair ability of cells against UVR (Sobrino et al.,
387 2008;Litchman et al., 2002). Phytoplankton use several mechanisms to repair
388 UV-induced damage, many of which involve N-requiring enzymes and/or protein
389 cofactors (Litchman et al., 2002). Korbee et al. (2010) reported that UVA could
390 stimulate algae N metabolism (nitrate transport and reductase activity). In contrast,
391 UVB was found to damage cell membranes and negatively affect nitrogen
392 incorporation mechanisms, leading to an increase in C/N ratio (Sobrino et al., 2004).
393 Subsequently, such a lack of nitrogen would inhibit essential protein turnover. In our
394 study at 24 °C, UVA and HC might act synergistically to maintain lower C/N ratio and
395 support the synthesis of UV-repair proteins, thereby partially counteracting the

396 UV-induced damage. As mentioned above, at 24 °C HC-grown cells were already
397 thermally inhibited, which may add the detrimental effect of UVB on nitrogen
398 assimilation and lead to much higher inhibition of photosynthesis by UVB in high
399 CO₂, warmer conditions.

400 When assessing the effect of UV radiation on calcification, we found that UVA
401 stimulated calcification rate of *E. huxleyi* PML B92/11, while UVB inhibited it. In
402 earlier studies, Gao et al. (2009) reported that both UVA and UVB negatively affected
403 calcification of *E. huxleyi* CS-369. One possibility for this discrepancy between our
404 studies can be attributed to strain-specific responses. On the other hand, the different
405 irradiances used by the two studies could be involved, as the light intensity used by
406 Gao et al. (2009) was over twice as high as the one we used. Like our study, Xu and
407 Gao (2015) also observed that moderate levels of UVR increased PIC production rates.
408 It has been demonstrated that *E. huxleyi* can use only bicarbonate to support its
409 calcification (Kottmeier et al., 2016; Paasche, 2002). The observed stimulation of
410 calcification by UVA can thus perhaps be attributed to UVA-enhanced bicarbonate
411 utilization (Xu and Gao, 2010)

412 Given that the responses of coccolithophore strains to environmental change can be
413 different depending on that strain's temperature optimum (Sett et al., 2014), the
414 temperatures we chose in this study were below, close or above optimum for *E.*
415 *huxleyi* growth based on its thermal tolerance curves. The lower temperature of 15 °C
416 that we used was around the mean summer surface water temperature in the region
417 where *E. huxleyi* PML B92/11 was isolated (Fielding, 2013). 20 °C on the other hand
418 represents a future warmer condition, with 24 °C being likely similar to the upper
419 limit of temperatures that will be experienced by this strain due to temperature
420 fluctuations in the future. In the present study, we found that UV radiation could

421 interact with both temperature and CO₂ concentration to alter their effects on
422 photosynthesis and calcification, thus changing Cal/Pho ratios. The interactive effects
423 of elevated CO₂ and UV radiation on non-calcifying marine organism have been
424 extensively reported (Li et al., 2012;Gao et al., 2012). With regard to the calcifying
425 coccolithophore *E.huxleyi*, ocean acidification generally reduces their calcification
426 (thinner coccolith layer) as well as the Cal/Pho ratio, based on a number of indoor
427 laboratory experiments with UV-free light sources (Tong et al., 2018). In the present
428 study, with increasing temperature, we found that there was no significant difference
429 for Cal/Pho ratios between high and low CO₂-grown cells under UV radiation at
430 24 °C. The light intensity used was equivalent to the mean light level in the upper
431 mixed layer (UML) based on time series station (19 °N, 118.5 °E) measurements in
432 the South China Sea. Our results imply that *E. huxleyi* exposed to moderate levels of
433 solar radiation can sustain their cell density with a constant Cal/Pho ratio under
434 progressive warming and acidification. However, considering the slow mixing of the
435 upper layer during the daytime, cells dwelling in a shallower UML are likely to be
436 exposed to higher doses of solar irradiances. Under such circumstances, UV radiation
437 is most likely to reduce Cal/Pho ratios in *E. huxleyi*, and ocean acidification will
438 exacerbate the effect of UV radiation (Gao et al., 2009). As a result, the net effects of
439 temperature, CO₂ concentration and UV radiation will largely depend on the levels of
440 solar radiation to which the cells are exposed.

441 In previous studies, most indoor laboratory experiments neglected the effects of UV
442 radiation due to the common use of UV-free light sources or UV-opaque vessels. Our
443 results demonstrated that UV radiation could greatly influence the combined effects of
444 future CO₂ enrichment and sea surface warming on the physiological performance of

445 *E. huxleyi*. Thus, the impacts UV radiation should be considered in order to build
446 more realistic predictions of future biological and biogeochemical processes in a high
447 CO₂ ocean.

448
449 **Author contributions:** S.T. and K.G. designed the study. The experiment was
450 performed by S.T. S.T., K.G. and D.H. contributed to the data analysis and manuscript
451 writing.

452 **Competing interests:** the authors declare that they have no conflict of interest.

453
454 **Acknowledgements:** This study was supported by National Natural Science
455 Foundation (41720104005, 41721005, 41430967), Joint Project of National Natural
456 Science Foundation of China and Shandong province (No. U1606404), U.S. National
457 Science Foundation grants OCE 1538525 and OCE 1638804, and Shandong
458 Provincial Natural Science Foundation (ZR2017QD007).

459
460
461
462 **References**

463
464 Alexiadis, A.: Global warming and human activity: A model for studying the potential
465 instability of the carbon dioxide/temperature feedback mechanism, *Ecol. Modell.*, 203,
466 243-256, 10.1016/j.ecolmodel.2006.11.020, 2007.

467 Cai, W.-J., Hu, X., Huang, W.-J., Murrell, M. C., Lehrter, J. C., Lohrenz, S. E., Chou,
468 W.-C., Zhai, W., Hollibaugh, J. T., and Wang, Y.: Acidification of subsurface coastal
469 waters enhanced by eutrophication, *Nature Geoscience*, 4, 766-770,
470 10.1038/ngeo1297, 2011.

471 Chen, C.-C., Shiah, F.-K., Chung, S.-W., and Liu, K.-K.: Winter phytoplankton

472 blooms in the shallow mixed layer of the South China Sea enhanced by upwelling, J.
473 Mar. Syst., 59, 97-110, 10.1016/j.jmarsys.2005.09.002, 2006.

474 Dickson, A. G.: Standard potential of the reaction: $\text{AgCl (s)} + 12\text{H}_2 \text{(g)} = \text{Ag (s)} + \text{HCl}$
475 (aq), and the standard acidity constant of the ion HSO_4^- in synthetic sea water
476 from 273.15 to 318.15 K, The Journal of Chemical Thermodynamics, 22, 113-127,
477 10.1016/0021-9614(90)90074-Z, 1990.

478 Feng, Y., Warner, M. E., Zhang, Y., Sun, J., Fu, F.-X., M. Rose, J., and Hutchins, D. A.:
479 Interactive effects of increased pCO_2 , temperature and irradiance on the marine
480 coccolithophore *Emiliana huxleyi* (Prymnesiophyceae), Eur. J. Phycol., 43, 87-98,
481 10.1080/09670260701664674, 2008.

482 Fielding, S. R.: *Emiliana huxleyi* specific growth rate dependence on temperature,
483 Limnol. Oceanogr., 58, 663-666, 10.4319/lo.2013.58.2.0663 2013.

484 Gao, K., Wu, Y., Li, G., Wu, H., e, V. E. V., and Helbling, E. W.: Solar UV Radiation
485 Drives CO_2 Fixation in Marine Phytoplankton: A Double-Edged Sword, Plant
486 Physiol., 144, 54-59, 10.1104/pp.107.098491, 2007.

487 Gao, K., Ruan, Z., Villafan, V. E., Gattuso, J.-P., and Helbling, E. W.: Ocean
488 acidification exacerbates the effect of UV radiation on the calcifying phytoplankter
489 *Emiliana huxleyi*, Limnol. Oceanogr., 54, 1855-1862, 10.4319/lo.2009.54.6.1855
490 2009.

491 Gao, K., Helbling, E. W., Häder, D.-P., and Hutchins, D. A.: Responses of marine
492 primary producers to interactions between ocean acidification, solar radiation, and
493 warming, Mar. Ecol.: Prog. Ser., 470, 167-189, 10.3354/meps10043, 2012.

494 Gattuso, J.-P., Pichon, M., and Frankignoulle, M.: Biological control of air-sea CO_2
495 fluxes: effect of photosynthetic and calcifying marine organisms and ecosystems,
496 Oceanographic Literature Review, 7, 663-664, 10.3354/meps129307, 1996.

497 Gattuso, J.-P., Magnan, A., Billé R., Cheung, W. W. L., Howes, E. L., Joos, F.,
498 Allemand, D., Bopp, L., Cooley, S. R., Eakin, C. M., Hoegh-Guldberg, O., Kelly, R.
499 P., Pörtner, H.-O., Rogers, A. D., Baxter, J. M., Laffoley, D., Osborn, D., Rankovic, A.,
500 Rochette, J., Sumaila, U. R., Treyer, S., and Turley, C.: Contrasting futures for ocean
501 and society from different anthropogenic CO_2 emissions scenarios, Science, 349,

502 10.1126/science.aac4722, 2015.

503 Guan, W., and Gao, K.: Impacts of UV radiation on photosynthesis and growth of the
504 coccolithophore *Emiliana huxleyi* (Haptophyceae), *Environ. Exp. Bot.*, 67, 502-508,
505 10.1016/j.envexpbot.2009.08.003, 2009.

506 Häder, D.-P., Williamson, C. E., Wängberg, S.-Å., Rautio, M., Rose, K. C., Gao, K.,
507 Helbling, E. W., Sinha, R. P., and Worrest, R.: Effects of UV radiation on aquatic
508 ecosystems and interactions with other environmental factors, *Photochemical &*
509 *Photobiological Sciences*, 10(2), 113-150, 10.1039/c4pp90035a, 2014.

510 Häder, D.-P., and Gao, K.: Interactions of anthropogenic stress factors on marine
511 phytoplankton, *Frontiers in Environmental Science*, 3, 1-14,
512 10.3389/fenvs.2015.00014, 2015.

513 Helbling, E. W., Gao, K., Gonçalves, R. J., Wu, H., and Villafañe, V. E.: Utilization of
514 solar UV radiation by coastal phytoplankton assemblages off SE China when exposed
515 to fast mixing, *Mar. Ecol. Prog. Ser.*, 259, 59-66, 10.3354/meps259059, 2003.

516 Helbling, E. W., Buma, A. G. J., Boelen, P., Strate, H. J. v. d., Giordanino, M. V. F.,
517 and Villafañe, V. E.: Increase in Rubisco activity and gene expression due to elevated
518 temperature partially counteracts ultraviolet radiation-induced photoinhibition in the
519 marine diatom *Thalassiosira weissflogii*, *Limnol. Oceanogr.*, 56, 1330-1342,
520 10.4319/lo.2011.56.4.1330, 2011.

521 Hutchins, D. A., and Fu, F.: Microorganisms and ocean global change, *Nature*
522 *Microbiology*, 2, 17058, 10.1038/nmicrobiol.2017.58, 2017.

523 Jin, P., Ding, J., Xing, T., Riebesell, U., and Gao, K.: High levels of solar radiation
524 offset impacts of ocean acidification on calcifying and non-calcifying strains of
525 *Emiliana huxleyi*, *Mar. Ecol.: Prog. Ser.*, 568, 47-58, 10.3354/meps12042 2017.

526 Korbee, N., Mata, M. T., and Figueroa, F. I. L.: Photoprotection mechanisms against
527 ultraviolet radiation in *Heterocapsa* sp. (Dinophyceae) are influenced by nitrogen
528 availability: Mycosporine-like amino acids vs. xanthophyll cycle, *Limnol. Oceanogr.*,
529 55, 899-908, 10.4319/lo.2010.55.2.0899, 2010.

530 Kottmeier, D. M., Rokitta, S. D., and Rost, B.: Acidification, not carbonation, is the
531 major regulator of carbon fluxes in the coccolithophore *Emiliana huxleyi*, *New*

532 Phytol., 211, 126-137, 10.1111/nph.13885, 2016.

533 Langer, G., Nehrke, G., Probert, I., Ly, J., and Ziveri, P.: Strain-specific responses of
534 *Emiliana huxleyi* to changing seawater carbonate chemistry, Biogeosciences, 6,
535 2637-2646, 10.5194/bg-6-2637-2009 2009.

536 Lewis, E., Wallace, D., and Allison, L. J.: Program developed for CO₂ system
537 calculations, Carbon Dioxide Information Analysis Center, managed by Lockheed
538 Martin Energy Research Corporation for the US Department of Energy Tennessee,
539 1998.

540 Li, Y., Gao, K., Villafañe, V. E., and Helbling, E. W.: Ocean acidification mediates
541 photosynthetic response to UV radiation and temperature increase in the diatom
542 *Phaeodactylum tricornutum*, Biogeosciences, 9, 3931-3942, 10.5194/bg-9-3931-2012,
543 2012.

544 Litchman, E., Neale, P. J., and Banaszak, A. T.: Increased sensitivity to ultraviolet
545 radiation in nitrogen-limited dinoflagellates: Photoprotection and repair, Limnol.
546 Oceanogr., 47, 86-94, 10.4319/lo.2002.47.1.0086, 2002.

547 Menden-Deuer, S., and Lessard, E. J.: Carbon to volume relationships for
548 dinoflagellates, diatoms, and other protist plankton, Limnol. Oceanogr., 45, 569-579,
549 10.4319/lo.2000.45.3.0569, 2000.

550 Milner, S., Langer, G., Grelaud, M., and Ziveri, P.: Ocean warming modulates the
551 effects of acidification on *Emiliana huxleyi* calcification and sinking, Limnology and
552 Oceanography, 61, 1322-1336, 2016.

553 Monteiro, F. M., Bach, L. T., Brownlee, C., Bown, P., Rickaby, R. E., Poulton, A. J.,
554 Tyrrell, T., Beaufort, L., Dutkiewicz, S., and Gibbs, S.: Why marine phytoplankton
555 calcify, Science Advances, 2, e1501822, 2016.

556 Norberg, J.: Biodiversity and ecosystem functioning: A complex adaptive systems
557 approach, Limnol. Oceanogr., 49, 1269-1277, 10.4319/lo.2004.49.4_part_2.1269,
558 2004.

559 Paasche, E.: The effect of temperature, light intensity, and photoperiod on coccolith
560 formation, Limnol. Oceanogr., 13, 178-181, 10.4319/lo.1968.13.1.0178, 1968.

561 Paasche, E.: A review of the coccolithophorid *Emiliana huxleyi* (Prymnesiophyceae),

562 with particular reference to growth, coccolith formation, and
563 calcification-photosynthesis interactions, *Phycologia*, 40, 503-529,
564 10.2216/i0031-8884-40-6-503.1, 2002.

565 Raitos, D. E., Lavender, S. J., Pradhan, Y., Tyrrell, T., Reid, P. C., and Edwards, M.:
566 Coccolithophore bloom size variation in response to the regional environment of the
567 subarctic North Atlantic, *Limnol. Oceanogr.*, 51, 2122-2130,
568 10.4319/lo.2006.51.5.2122, 2006.

569 Raven, J. A., and Crawford, K.: Environmental controls on coccolithophore
570 calcification, *Mar. Ecol.: Prog. Ser.*, 470, 137-166, 10.3354/meps09993, 2012.

571 Riebesell, U., Zondervan, I., Rost, B., Tortell, P. D., Zeebe, R. E., and Morel, F. M. M.:
572 Reduced calcification of marine plankton in response to increased atmospheric CO₂,
573 *Nature*, 407, 364-367, 10.1038/35030078, 2000.

574 Riebesell, U., Bach, L. T., Bellerby, R. G. J., Monsalve, J. R. B., Boxhammer, T.,
575 Czerny, J., Larsen, A., Ludwig, A., and Schulz, K. G.: Competitive fitness of a
576 predominant pelagic calcifier impaired by ocean acidification, *Nature Geoscience*, 10,
577 19-24, 10.1038/NGEO2854, 2017.

578 Rost, B., and Riebesell, U.: Coccolithophores and the biological pump: responses to
579 environmental changes, in: *Coccolithophores*, Springer, 99-125, 2004.

580 Roy, R. N., Roy, L. N., Vogel, K. M., Porter-Moore, C., Pearson, T., Good, C. E.,
581 Millero, F. J., and Campbell, D. M.: The dissociation constants of carbonic acid in
582 seawater at salinities 5 to 45 and temperatures 0 to 45 C, *Marine Chemistry*, 44,
583 249-267, 1993.

584 Sett, S., Bach, L. T., Schulz, K. G., Koch-Klavsen, S., Lebrato, M., and Riebesell, U.:
585 Temperature modulates coccolithophorid sensitivity of growth, photosynthesis and
586 calcification to increasing seawater pCO₂, *Plos one*, 9, 1-9,
587 10.1371/journal.pone.0088308, 2014.

588 Sobrino, C., Montero, O., and Lubián, L. M.: UV-B radiation increases cell
589 permeability and damages nitrogen incorporation mechanisms in *Nannochloropsis*
590 *gaditana*, *Aquatic Sciences*, 66, 421-429, 10.1007/s00027-004-0731-8, 2004.

591 Sobrino, C., and Neale, P. J.: Short-term and long-term effects of temperature on

592 photosynthesis in the diatom *Thalassiosira Pseudonana* under UVR exposures, J.
593 Phycol., 43, 426-436, 10.1111/j.1529-8817.2007.00344.x, 2007.

594 Sobrino, C., Ward, M. L., and Neale, P. J.: Acclimation to elevated carbon dioxide and
595 ultraviolet radiation in the diatom *Thalassiosira pseudonana*: Effects on growth,
596 photosynthesis, and spectral sensitivity of photoinhibition, Limnol. Oceanogr., 53,
597 494-505, 10.4319/lo.2008.53.2.0494, 2008.

598 Stocker, T., Qin, D., Plattner, G.-K., Tignor, M., Allen, S. K., Boschung, J., Nauels, A.,
599 Xia, Y., Bex, V., and Midgley, P. M.: Climate change 2013: The physical science basis,
600 Cambridge University Press Cambridge, UK, and New York, 2014.

601 Sunda, W. G., Price, N. M., and Morel, F. M.: Trace metal ion buffers and their use in
602 culture studies, Algal culturing techniques, 4, 35-63, 10.1007/s13398-014-0173-7.2,
603 2005.

604 Tedetti, M., Sempéré R., Vasilkov, A., Charriere, B., Néini, D., Miller, W. L.,
605 Kawamura, K., and Raimbault, P.: High penetration of ultraviolet radiation in the
606 south east Pacific waters, Geophysical Research Letters, 34, L12610,
607 10.1029/2007GL029823, 2007.

608 Thomas, M. K., Kremer, C. T., Klausmeier, C. A., and Litchman, E.: A Global Pattern
609 of Thermal Adaptation in Marine Phytoplankton, Science, 338, 1085-1088,
610 10.1126/science.1224836, 2012.

611 Tong, S., Hutchins, D. A., Fu, F., and Gao, K.: Effects of varying growth irradiance
612 and nitrogen sources on calcification and physiological performance of the
613 coccolithophore *Gephyrocapsa oceanica* grown under nitrogen limitation, Limnol.
614 Oceanogr., 61, 2234-2242, 10.1002/lno.10371, 2016.

615 Tong, S., Gao, K., and Hutchins, D. A.: Adaptive evolution in the coccolithophore
616 *Gephyrocapsa oceanica* following 1,000 generations of selection under elevated CO₂,
617 Global Change Biol., 24, 3055-3064, 10.1111/gcb.14065, 2018.

618 Voss, K. J., Balch, W. M., and Kilpatrick, K. A.: Scattering and attenuation properties
619 of *Emiliana Huxleyi* cells and their detached coccoliths, Limnol. Oceanogr., 43,
620 870-876, 10.4319/lo.1998.43.5.0870, 1998.

621 Williamson, C. E., Zepp, R. G., Lucas, R. M., Madronich, S., Austin, A. T., Ballaré C.

622 L., Norval, M., Sulzberger, B., Bais, A. F., McKenzie, R. L., Robinson, S. A., Häder,
623 D.-P., Paul, N. D., and Bornman, J. F.: Solar ultraviolet radiation in a changing
624 climate, *Nature climate change*, 4, 434-441, 10.1038/nclimate2225, 2014.

625 Wu, Y., Gao, K., Li, G., and Helbling, E. W.: Seasonal Impacts of Solar UV Radiation
626 on Photosynthesis of Phytoplankton Assemblages in the Coastal Waters of the South
627 China Sea, *Photochem. Photobiol.*, 86, 586-592, 10.1111/j.1751-1097.2009.00694.x,
628 2010.

629 Xu, J., and Gao, K.: Use of UV-A Energy for Photosynthesis in the Red Macroalga
630 *Gracilaria lemaneiformis*, *Photochem. Photobiol.*, 86, 580-585,
631 10.1111/j.1751-1097.2010.00709.x, 2010.

632 Xu, J., Bach, L. T., Schulz, K. G., Zhao, W., and Gao, K.: The role of coccoliths in
633 protecting *Emiliana huxleyi* against stressful light and UV radiation, *Biogeosciences*,
634 13, 4637-4643, 10.5194/bg-13-4637-2016, 2016.

635 Xu, K., and Gao, K.: Solar UV Irradiances Modulate Effects of Ocean Acidification
636 on the Coccolithophorid *Emiliana huxleyi*, *Photochem. Photobiol.*, 91, 92-101,
637 10.1111/php.12363, 2015.

638

639

640

641

642

643

644

645

646

647

648

649

650

651 Table 1. Mean values of the seawater carbonate system parameters under HC (1000
 652 μatm) and LC (400 μatm) at 15, 20 and 24 °C. The cell concentrations of all cultures
 653 were maintained below 5×10^4 cells ml^{-1} and pH variations were <0.04 units. The
 654 superscripts represent significant difference between HC and LC ($p < 0.05$).

	Treatment	pH _{NBS}	DIC ($\mu\text{mol kg}^{-1}$)	pCO ₂ (μatm)	HCO ₃ ⁻ ($\mu\text{mol kg}^{-1}$)	CO ₃ ²⁻ ($\mu\text{mol kg}^{-1}$)	Total alkalinity ($\mu\text{mol kg}^{-1}$)
15 °C	HC	7.80 ± 0.02 ^a	2147.2 ± 105.7 ^a	1000 ± 40 ^a	2037.5 ± 98.6 ^a	72.4 ± 7 ^a	2228.5 ± 114.4 ^a
	LC	8.13 ± 0.01 ^b	1919.2 ± 27.2 ^b	400 ± 40 ^b	1768.1 ± 23.6 ^b	136.2 ± 3.6 ^b	2122.8 ± 31.7 ^a
20 °C	HC	7.82 ± 0.01 ^a	2153.2 ± 57.3 ^a	1000 ± 40 ^a	2031.5 ± 52.8 ^a	89.74 ± 4.5 ^a	2262.7 ± 62.9 ^a
	LC	8.16 ± 0.01 ^b	1961.8 ± 25.7 ^b	400 ± 40 ^b	1777.8 ± 21.8 ^b	170.13 ± 3.9 ^b	2214.38 ± 30.4 ^a
25 °C	HC	7.84 ± 0.01 ^a	2057.2 ± 28.1 ^a	1000 ± 40 ^a	2174.8 ± 26.2 ^a	106.3 ± 2.5 ^a	2310.3 ± 31.2 ^a
	LC	8.18 ± 0.01 ^b	1854.6 ± 46.5 ^b	400 ± 40 ^b	1999.8 ± 38.4 ^b	203.1 ± 8.2 ^b	2297.2 ± 56.4 ^a

655

656

657

658

659

660

661

662

663

664

665

666 Table 2. The optimal temperature for growth (T_{opt}) and the maximum growth rate
667 (μ_{max}) at T_{opt} of *E. huxleyi* grown in 400 μatm (LC) and 1000 μatm (HC) CO_2
668 concentrations. T_{opt} and μ_{max} as estimated from the fitted curves in Fig. 1 by numerical
669 optimization.

	T_{opt} ($^{\circ}\text{C}$)	μ_{max} (μ)
HC	20.58	1.22
LC	22.15	1.31

670

671

672

673

674

675

676

677

678

679

680

681

682

683

684

685

686 Table 3. Three-way ANOVA analyses of interactive effects among pCO₂ (CO₂),
687 temperature (T), and irradiance (I, including P, PA and PAB) on photosynthetic carbon
688 fixation rates, calcification rates and Cal/Pho ratios respectively. Also shown are
689 three-way ANOVA analyses of interactive effects among CO₂ (CO₂), temperature (T)
690 and irradiance (I, including UVA, UVB and UVR) on the inhibition of photosynthesis,
691 calcification and Cal/Pho ratios respectively. “*” and “**” represent significance
692 levels at p<0.05 and 0.01 respectively.

	T×I <i>p</i> (df, F)	T×CO ₂ <i>p</i> (df, F)	I×CO ₂ <i>p</i> (df, F)	T×I×CO ₂ <i>p</i> (df, F)
Pho rate	<0.01** (4, 7.220)	<0.01** (2, 11.505)	0.042* (2, 3.453)	0.055 (4, 2.560)
Cal rate	0.018* (4, 3.432)	0.541 (2, 0.625)	0.465 (2, 0.783)	0.483 (4, 0.885)
Cal/Pho ratio	<0.01** (4, 8.253)	0.03* (2, 3.874)	0.632 (2, 0.464)	0.002** (4, 5.155)
Inh of Pho rate	0.231 (4, 1.473)	0.381 (2, 0.991)	0.565 (2, 0.580)	<0.01** (4, 8.546)
Inh of cal rate	0.01** (4, 3.928)	0.24 (2, 1.484)	<0.01** (2, 8.881)	<0.01** (4, 6.610)
Inh of Cal/Pho ratio	0.021* (4, 3.331)	0.108 (2, 2.365)	0.127 (2, 2.186)	<0.01** (4, 6.727)

693

694

695

696

697

698

699

700

701 Fig. 1 Thermal reaction norms of *E. huxleyi* grown in 400 μatm (LC) and 1000 μatm
702 (HC) CO_2 concentrations. Corresponding $R^2=0.996$ (LC) and 0.999 (HC), respectively.
703 The values are the means and the error bars are standard deviations for triplicate
704 cultures at each treatment.

705 Fig. 2 Specific growth rate of *E. huxleyi* grown in 400 μatm (LC) and 1000 μatm (HC)
706 CO_2 concentrations at 15 $^\circ\text{C}$, 20 $^\circ\text{C}$ and 24 $^\circ\text{C}$ respectively. The different letters above
707 the bars indicate significant differences among the treatments ($p<0.05$). The values are
708 the means and the error bars are standard deviations for triplicate cultures at each
709 treatment.

710 Fig. 3 Cellular POC (a), cellular PIC (b), POC production rate (c), PIC production rate
711 (d), inner coccosphere volume (e) and PIC/POC ratio (f) of *E. huxleyi* grown in 400
712 μatm (LC) and 1000 μatm (HC) CO_2 concentrations at 15 $^\circ\text{C}$, 20 $^\circ\text{C}$ and 24 $^\circ\text{C}$
713 respectively. The different letters above the bars indicate significant differences
714 among the treatments ($p<0.05$). The values are the means and the error bars are
715 standard deviations for triplicate cultures at each treatment.

716 Fig. 4 Cellular PON content (a) and C/N ratio (b) of *E. huxleyi* grown in 400 μatm
717 (LC) and 1000 μatm (HC) CO_2 concentrations at 15 $^\circ\text{C}$, 20 $^\circ\text{C}$ and 24 $^\circ\text{C}$ respectively.
718 The different letters above the bars indicate significant differences among the
719 treatments ($p<0.05$). The values are the means and the error bars are standard
720 deviations for triplicate cultures at each treatment.

721 Fig. 5 Photosynthetic carbon fixation rates (a, b, c) under P (irradiance above 395
722 nm), PA (irradiance above 320 nm) and PAB (irradiance above 295 nm), and

723 inhibition of photosynthetic carbon fixation rates (d, e, f) due to UVA, UVB and UVR
724 of *E. huxleyi* in HC- and LC-grown cells at 15, 20 and 25 °C . Lines above the
725 histogram bars indicate significant differences between the HC and LC treatments,
726 and different letters indicate significant differences among the radiation treatments
727 within the HC or LC-grown cells within each panel.

728 Fig. 6 Calcification rates under P, PA and PAB (a, b, c); inhibition of calcification
729 rates due to UVA, UVB and UVR (d, e, f); and Cal/Pho ratios under P, PA and PAB (g,
730 h, i) for *E. huxleyi* in HC- and LC-grown cells at 15, 20 and 24 °C. Negative
731 inhibition values indicate stimulation. Lines above the histogram bars indicate
732 significant differences between the HC and LC treatments, and different letters
733 indicate significant differences among the radiation treatments within the HC or
734 LC-grown cells within each panel.

735

736

737

738

739

740

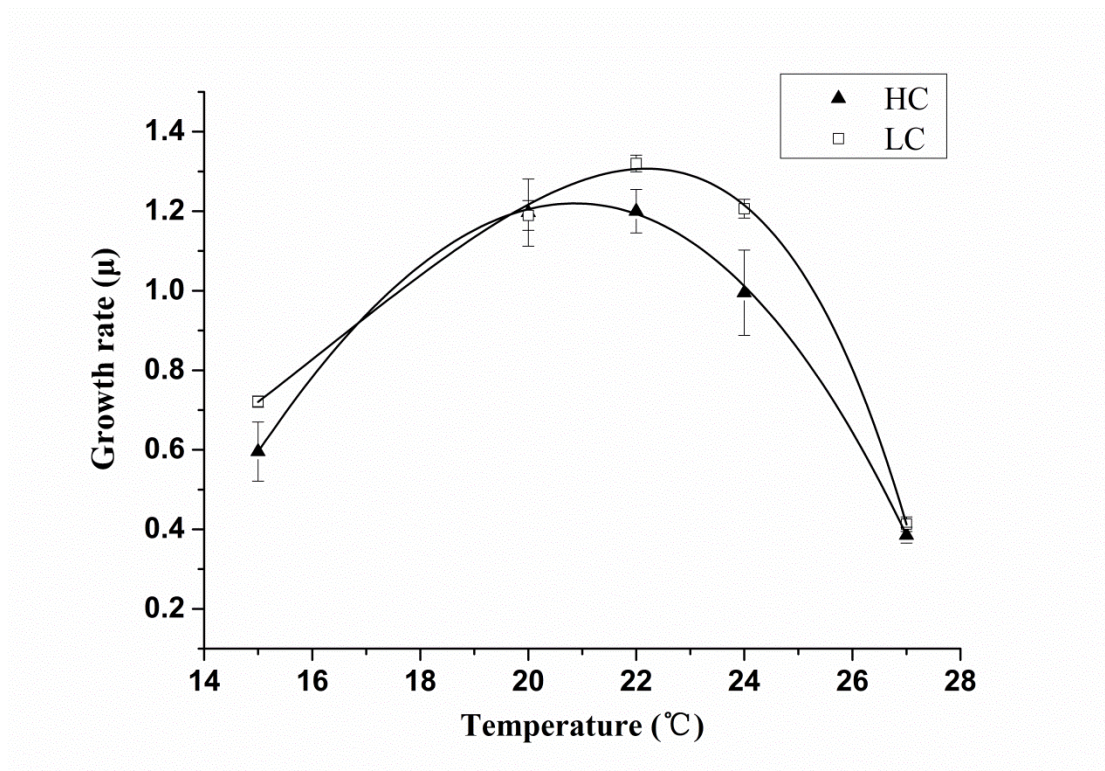
741

742

743

744

745 Fig. 1



746

747

748

749

750

751

752

753

754

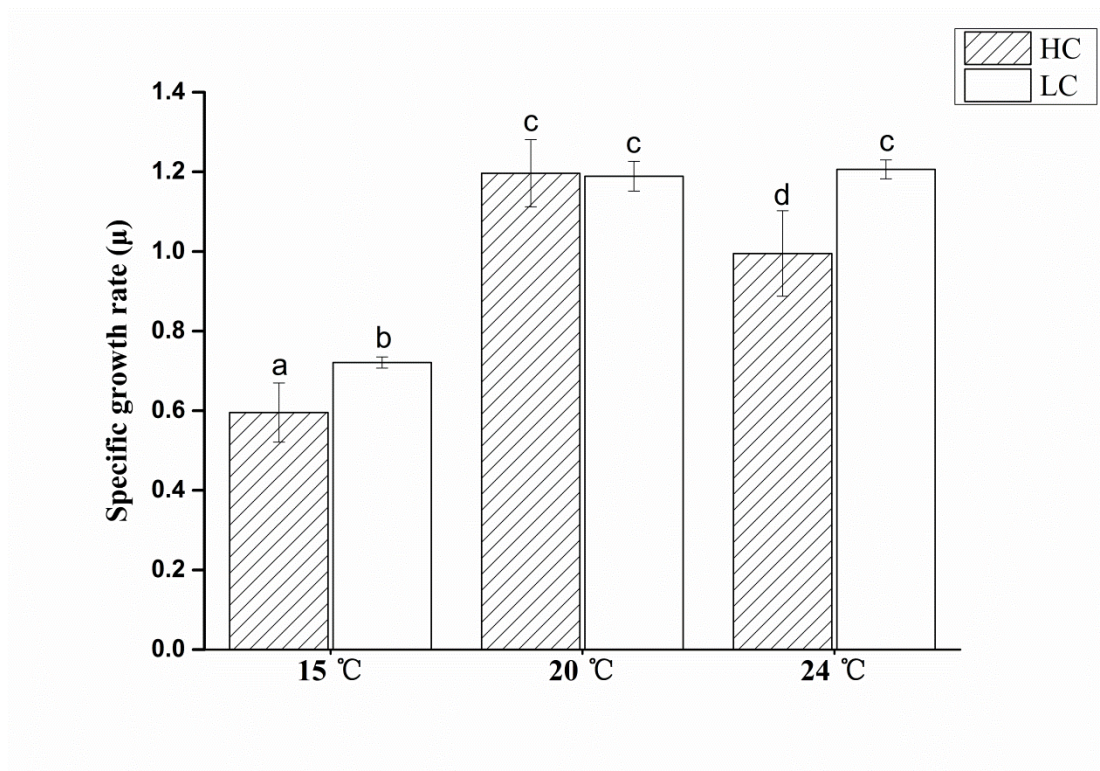
755

756

757

758

759 Fig. 2



760

761

762

763

764

765

766

767

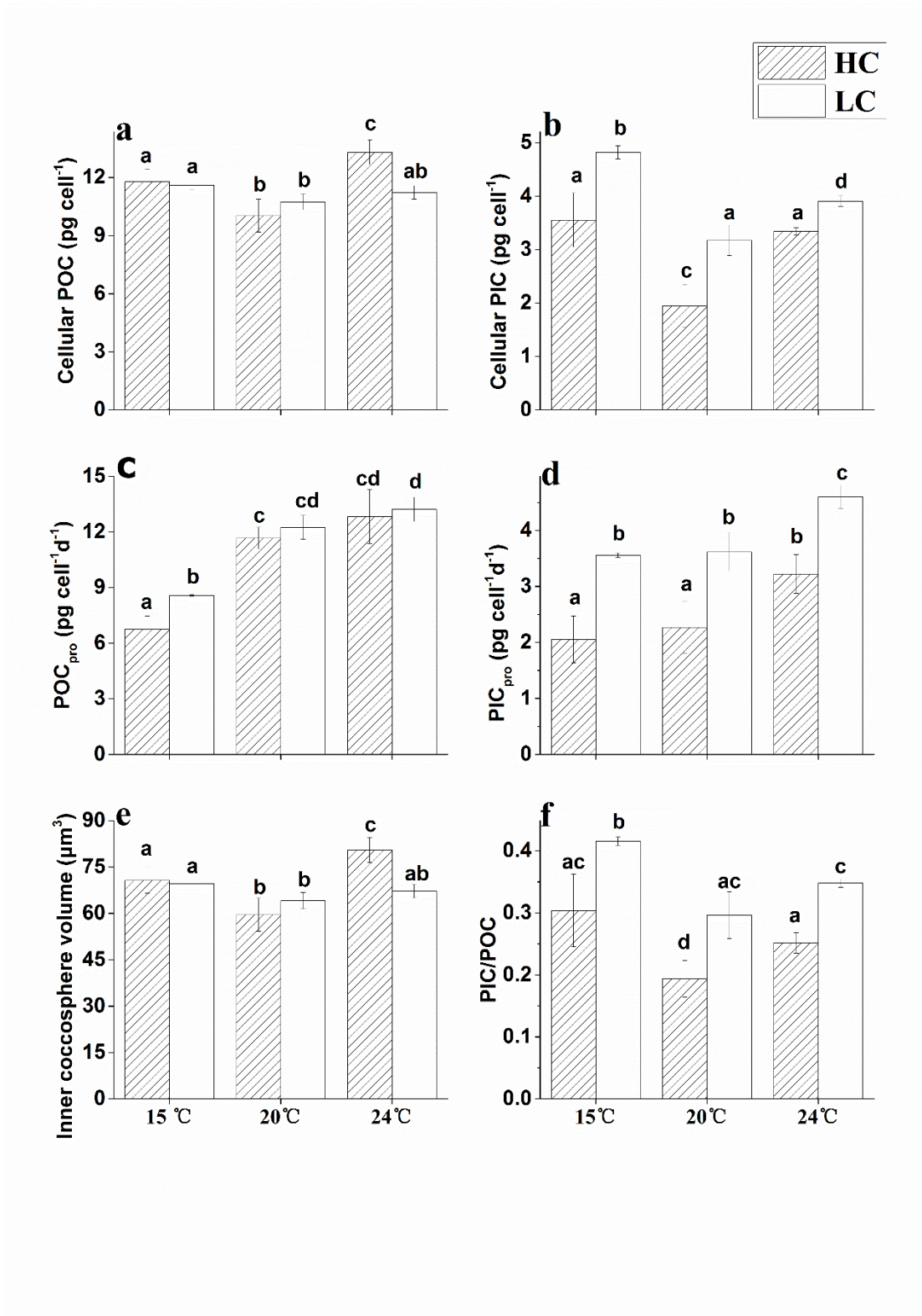
768

769

770

771

772



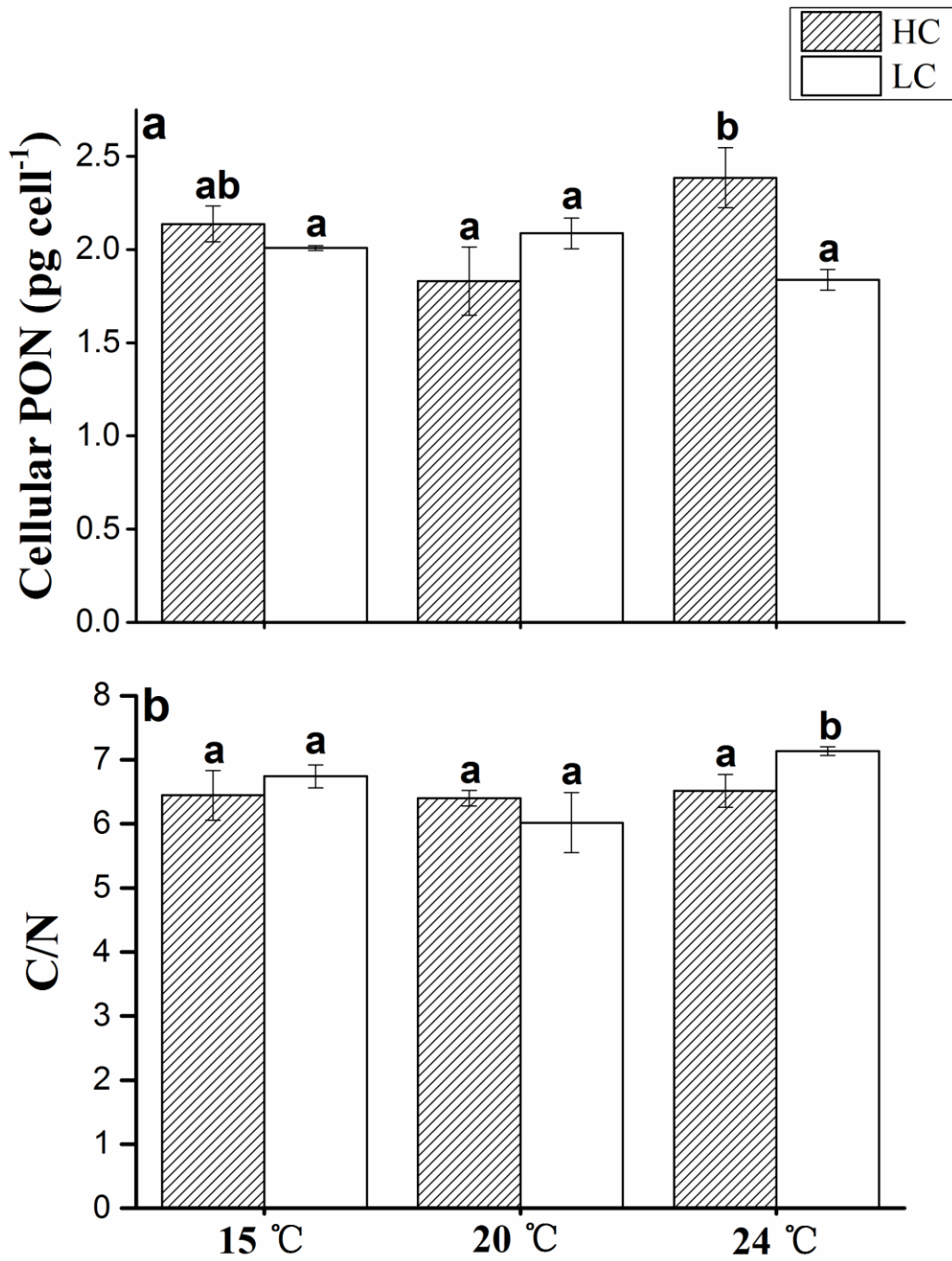
774

775

776

777 Fig. 4

778

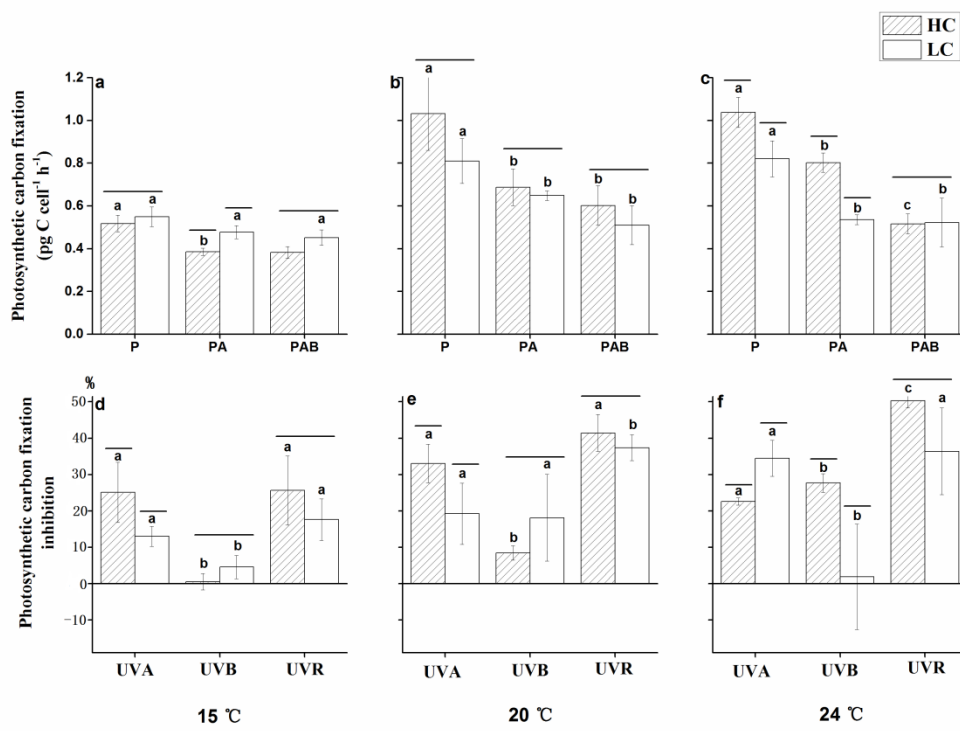


779

780

781 Fig. 5

782



783

784

785

786

787

788

789

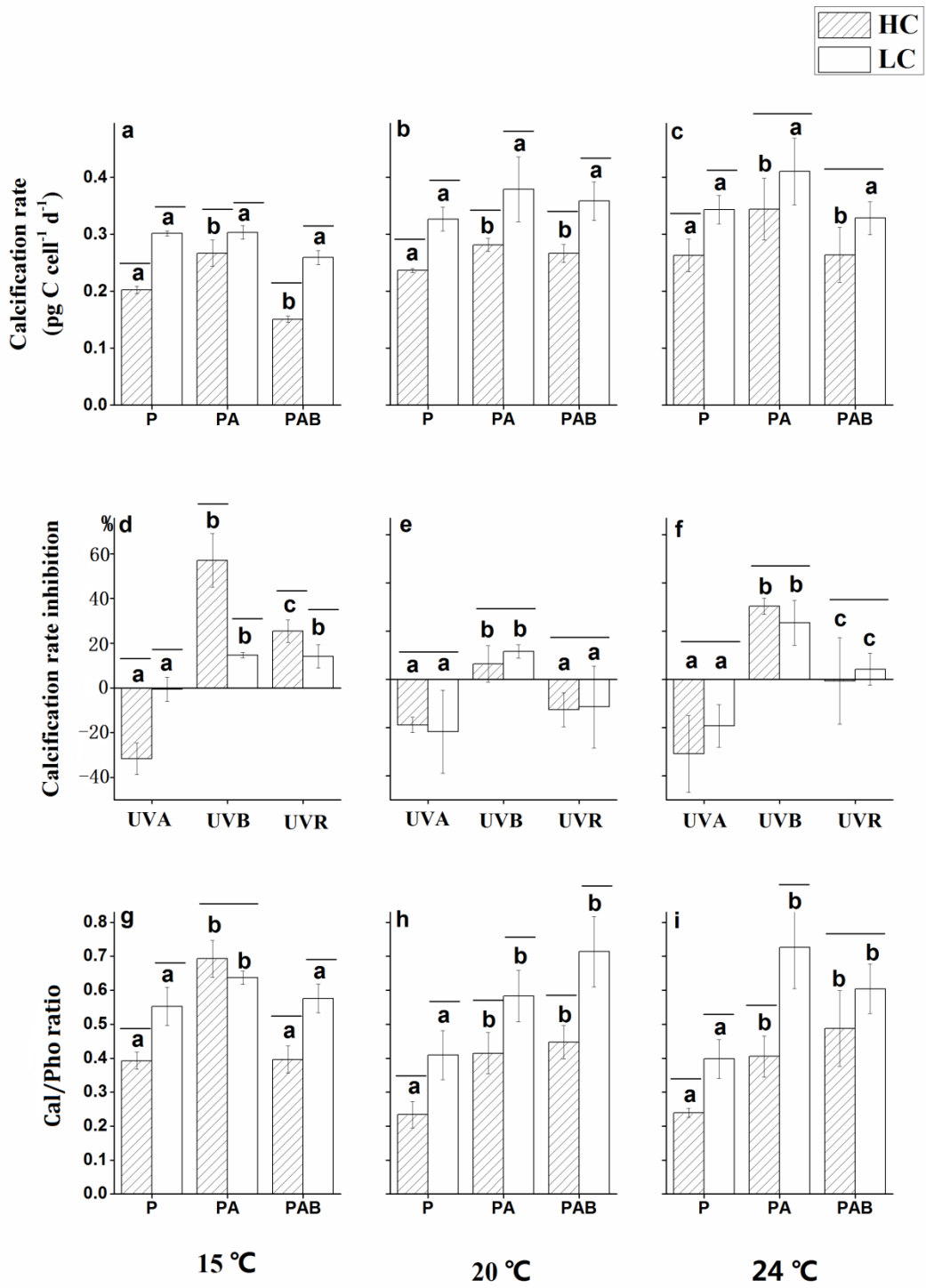
790

791

792

793

794



796

797

798